Thermodynamic-Kinetic Synergistic Separation of CH4/N2 on A Robust Aluminum-Based Metal-Organic Framework

Feifei Zhang[1], Hua Shang[1], Bolun Zhai[1], Xiaoming Li[1], Yingying Zhang[1], Xiaoqing Wang[1], jinping Li[1], and Jiangfeng Yang[1]

[1]Taiyuan University of Technology

November 3, 2022

Abstract

A robust aluminum-based metal-organic framework (Al-MOF) MIL-120Al with 1D rhombic ultra-microporous was reported. The non-polar porous walls composed of para-benzene rings with a comparable pore size to the kinetic diameter of methane allow it to exhibit a novel thermodynamic-kinetic synergistic separation of CH4/N2 mixtures. The CH4 adsorption capacity was as high as 33.7 cm3/g (298 K, 1 bar), which is the highest uptake value among the Al-MOFs reported to date. The diffusion rates of CH4 were faster than N2 in this structure as confirmed by time-dependent kinetic adsorption profiles. Breakthrough experiments confirm that this MOF can completely separate the CH4/N2 mixture and the separation performance is not affected in the presence of H2O. Theoretical calculations reveal that pore centers with more energetically-favorable binding sites for CH4 than N2. The results of pressure swing adsorption (PSA) simulations indicate that MIL-120Al is a potential candidate for selective capture coal-mine methane.

Thermodynamic-Kinetic Synergistic Separation of CH_4/N_2 on A Robust Aluminum-Based Metal-Organic Framework

Feifei Zhang[1], Hua Shang[1], Bolun Zhai[1], Xiaoming Li[1], Yingying Zhang[1], Xiaoqing Wang[1], Jinping Li[1,2,3], Jiangfeng Yang[*1,2],

[1] Research Institute of Special Chemicals, College of Chemistry and Chemical Engineering, Taiyuan University of Technology, Taiyuan 030024, Shanxi, P. R. China.

[2] Shanxi Key Laboratory of Gas Energy Efficient and Clean Utilization, Taiyuan 030024, Shanxi, P. R. China.

[3] Shanxi-Zheda Institute of Advanced Materials and Chemical Engineering, Taiyuan 030002, Shanxi, China.

Correspondence

Jiangfeng Yang, Research Institute of Special Chemicals, College of Chemistry and Chemical Engineering, Taiyuan University of Technology, Taiyuan 030024, Shanxi, P. R. China.

E-mail:*yangjiangfeng@tyut.edu.cn*

Abstract

A robust aluminum-based metal-organic framework (Al-MOF) MIL-120Al with 1D rhombic ultra-microporous was reported. The non-polar porous walls composed of para-benzene rings with a comparable pore size to the kinetic diameter of methane allow it to exhibit a novel thermodynamic-kinetic synergistic separation of CH_4/N_2 mixtures. The CH_4 adsorption capacity was as high as 33.7 cm^3/g (298 K, 1 bar), which is the highest uptake value among the Al-MOFs reported to date. The diffusion rates of CH_4 were faster than N_2 in this structure as confirmed by time-dependent kinetic adsorption profiles. Breakthrough experiments confirm that this MOF can completely separate the CH_4/N_2 mixture and the separation performance is not affected in the presence of H_2O. Theoretical calculations reveal that pore centers with more energetically-favorable binding sites for CH_4 than N_2. The results of pressure swing adsorption (PSA) simulations indicate that MIL-120Al is a potential candidate for selective capture coal-mine methane.

KEYWORDS

Coal-mine methane, metal-organic framework, CH_4/N_2 separation, thermodynamic-kinetic synergistic separation, PSA simulation

1 INTRODUCTION

Due to the continuous and increasing use of traditional fossil fuels, the world is facing great challenges in terms of the energy crisis and environmental problems.[1,2] Natural gas (mainly methane), which has a high combustion calorific value, is regarded as a promising alternative to traditional fossil fuels.[3,4] To date, the consumption of natural gas has occupied an important proportion of primary energy consumption (24.2%) and is still growing.[5] To meet the ever-growing for demand natural gas, it is of great significance to seek more gas sources in addition to conventional gas reservoirs. As a vital component of unconventional natural gas, coal-mine methane (CMM) has been shown to contain a large amount of methane. There are ˜29 to 41 billion cubic meters of CMM liberated from underground coal mines every year, which can complement conventional natural gas supplies.[6] However, removing the unacceptable concentrations of impurities in CMM is an important prerequisite before its commercial use, especially nitrogen.[7-10]

Currently, cryogenic distillation based on the boiling point difference (112 K for CH_4 and 77 K for N_2) is utilized as the main technology for CMM enrichment, but the high energy consumption and operation cost hinder its industrial application.[11,12] To overcome these issues, adsorption-based technology is regarded as a promising strategy benefiting from its low investment cost, simple operation, flexibility, and energy conservation. However, the key to this technology is the availability of high-performance adsorbents.[13,14] Unfortunately, the adsorption/separation of CH_4/N_2 is particularly difficult due to their similar kinetic diameters (3.8 Å for CH_4 and 3.6 Å for N_2) and comparable polarizability (CH_4: 26.0 × $10^{-25} cm^3$ and N_2: 17.6 x 10^{-25} cm^3).[8,10] Traditional adsorbents including activated carbons and zeolites have been investigated for CH_4/N_2 separation, but their industrialization remains a distant option, which is limited by their low selectivity and/or poor capacity.[8] Considering the urgency of CH_4/N_2 separation, new types of adsorbents, which are industrially feasible, need to be developed.

As a new type of crystalline porous material, metal–organic frameworks (MOFs) have exhibited potential application in the field of gas adsorption and separation.[15-17] Due to their designability and structural and chemical adjustability, MOFs provide the opportunity to design of new materials with better gas separation performance.[18-26] In regard to CH_4/N_2 separation, MOFs have been proven to possess high-efficiency separation performance.[12,27] For example, ATC-Cu reported by Ma and co-workers exhibited a new CH_4 capture benchmark of 64.9 cm^3/g due to its high-density open Cu sites.[12] More recently, $Ni(ina)_2$ was observed to possess the highest ever reported CH_4/N_2 selectivity of 15.8 under ambient conditions.[27] It is worth noting that although many MOFs show high IAST selectivity and CH_4 uptake, most of them cannot meet the demands of practical industrial application and hindered due to their high toxicity, scarcity, and use of expensive metal salts and/or organic ligands, as well as poor thermal and chemical stability. Al-MOFs, which are constructed from AlO_6 polyhedra and an organic carboxylate linker are considered to be one of the most prospective materials for CH_4/N_2 separation in practical applications.[28] Due to their high structural stability and large-scale synthesis, Al-MOFs are easy to commercialize.[29] Al-BDC (Basolite A100) and Al-

FUM (Basolite A520) have been commercialized by BASF SE. Consequently, it is necessary to discover new Al-MOFs with prominent CH_4/N_2 separation properties from the viewpoint of their industrial application.

Current studies on CH_4/N_2 separation have mostly focused on MOF materials with ultra-microporous structures (<7 A) and non-polar/inert pore environments, which are mainly considered from the perspective of thermodynamic separation.[1,2,12,27,30] In fact, the separation performance of adsorbents is affected by both thermodynamic and kinetic factors. Previous studies have proven that the adsorption kinetic behavior will play an important role when the pore size of the adsorbent is comparable to the kinetic diameter of the target gas,[31-35] and sometimes exhibit a size sieve effect.[36-39] Bearing this analysis in mind, it can be predicted that Al-MOFs will display both priority CH_4dynamic and thermodynamic adsorption behavior and exhibit excellent CH_4/N_2 separation performance under dynamic conditions.

Herein, we studied an ultra-microporous MOF (MIL-120Al) with non-polar pore walls composed of para-benzene rings with a comparable pore size to the kinetic diameter of methane, which exhibits the thermodynamic-kinetic synergistic separation of CH_4/N_2 mixtures. Single-component adsorption isotherms and time-dependent kinetic adsorption studies on CH_4 and N_2 were carried out. Our results show the remarkable diffusivity and adsorption difference between CH_4 and N_2. The high CH_4/N_2 separation performance was confirmed using breakthrough experiments and pressure swing adsorption (PSA) process simulations. More importantly, this MOF can be easily regenerated and synthesized on a large-scale, and exhibits ultra-high chemical and thermal stability.

2 EXPERIMENTAL DETAILS

2.1 Materials

Aluminum nitrate nonahydrate ($Al(NO_3)_3$*$9H_2O$, 99%) and 1,2,4,5-benzenetetracarboxylic acid (BTEC, 98%) were purchased from Shanghai Aladdin Biochemical Technology Co., Ltd. Sodium hydroxide (NaOH, 99%) and methanol (CH_3OH, 99%) were provided by Sinopharm Chemical Reagent Co., Ltd. The above reagents were used directly without further purification. The distilled water used in our experiments was prepared in our laboratory.

The synthesis and purification of MIL-120Al were performed according to a previously reported method with some modifications.[40] The synthesis process was as follows: $Al(NO_3)_3$*$9H_2O$ (3.2 g, 8.5 mmol) and BTEC (0.5 g, 2.0 mmol) were added to a 100 mL polytetrafluoroethylene reaction kettle and 20 mL of water added using a pipette. The above mixture was stirred at 298 K for 20 min. NaOH (0.54 g, 13.6 mmol) was added to the resulting mixture and stirring continued at 298 K for 20 min. The resulting mixture was sealed in a stainless-steel shell and placed in an oven. The oven temperature was increased from room temperature to 473 K within 2 h and kept at 473 K for 24 h. The reaction kettle was removed from the oven and allowed to cool naturally to the room temperature. The white powder was collected upon repeated centrifugation and thorough washing with 353 K distilled water and 423 K CH_3OH, and the product dried at room temperature.

A large-scale synthesis of MIL-120Al was carried out as follows: $Al(NO_3)_3$*$9H_2O$ (0.13 kg, 0.34 mol), BTEC (0.02 kg, 0.08 mol), and NaOH (0.02 kg, 0.56 mol) were dissolved in 0.8 L of deionized water. The solution was stirred for 30 min and then placed in a 2 L stainless steel reactor for synthesis at 473 K for 24 h. After cooling down to room temperature, the sample was filtered, washed with H_2O/CH_3OH (1/1, v/v) solution at 423 K three times, and dried at room temperature. The product was obtained with a yield of ˜40–45 g.

2.2 Characterization

The crystallinity of the MIL-120Al powder was studied using a Bruker D8 ADVANCE X-ray diffractometer employing Cu-Kα (λ = 1.5418 Å) radiation. Thermogravimetric analysis (TGA) of the samples was performed on a Netzsch STA 449 F5 (Germany) differential thermal analyzer under a nitrogen atmosphere. The temperature test range was 298–1073 K and the heating rate was 10 K/min. Scanning electron microscopy (SEM) was performed on a ZEISS Sigma 300 at an accelerating voltage of 5 kV.

2.3 Kinetic and equilibrium adsorption measurement

Kinetic adsorption profiles were measured on an Intelligent Gravimetric Analyzer (IGA001, Hiden, UK). N_2 and CH_4 single-component gas adsorption isotherms were measured on a Micromeritics APSP 2460 analyzer. The nitrogen and carbon dioxide adsorption and desorption isotherms of the samples were obtained at 77 and 195 K on a Micromeritics APSP 2020 analyzer. The samples were activated at 423 K and 1×10^{-5} mbar for 12 h prior to testing. All gases used were of 99.99% purity.

2.4 Transient breakthrough experiments

The breakthrough curves of MIL-120Al were obtained at 298–313 K at a CH_4/N_2 mixed gas flow rate of 10 mL/min. The adsorbent powders were first tableted under a pressure of 4 MPa using a tablet press and then sieved into particles with diameters of ˜2 mm using a stainless-steel screen. The prepared MIL-120Al (3.40 g) particles were activated at 423 K and 1×10^{-5} mbar for 12 h and then filled in an adsorption column (Φ 9.0×150 mm) under an environment free from water. Prior to starting the test, the adsorption column was flushed with He gas at a flow rate of 15 mL/min and 373 K. The inlet gas was then switched to the CH_4/N_2 mixture to be tested at a total gas flow of 10 mL/min. The component concentrations in the effluent gas were monitored using an online mass spectrometer (HPR-20 EGA, Hiden, UK, detection limit 0.01%). After each separation test, the adsorption bed was regenerated under a flow of He (15 mL/min) for 20 min at ambient temperature.

2.5 Theoretical calculations

GCMC simulations were carried out using the Sorption program (BIOVIA Material studio 2019) to investigate the interactions between the framework and gas molecules. In our work, the crystal structures of MIL-120Al were chosen for our related simulations without further geometry optimization. A cut-off radius of 18.5 Å was used to handle the non-bonding interactions and the Ewald & Group summation method was applied to calculate the long-range electrostatic interactions. Each state point of the GCMC simulations contained 1×10^7 steps to guarantee equilibration, followed by 1×10^7 steps to sample the required thermodynamics properties. The MOF frameworks were treated as rigid structures by fixing the atoms at their crystallographic positions, which has been proven to yield accurate results in a large variety of GCMC studies. COMPASSII force field was adopted to describe the interactions for the atoms in our simulations. The partial charges for all atoms were derived using the DFT method (GGA-PBE/DNP).[41]

2.6 Modeling and simulation of the PSA process

PSA process simulations (Figure S1) were carried out using our previously reported method.[42,43] The formulas required for the simulation are listed in the Table S9. To simplify the adsorption process and improve the calculation speed, six assumptions were followed in the simulations. More details can be found in the Supporting information.

3 RESULTS AND DISCUSSION
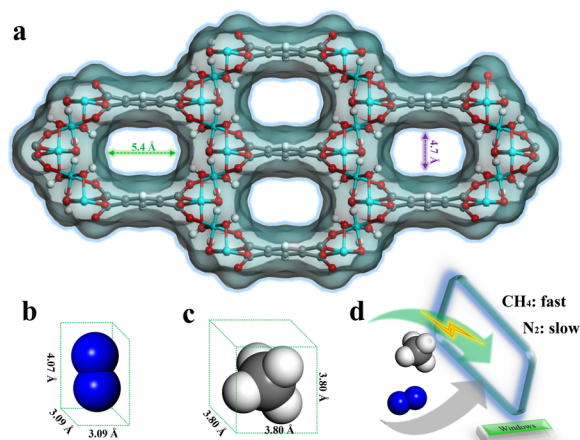
3.1 Characterization of MIL-120Al

FIGURE 1 (a) 3D framework of MIL-120Al; (b, c) molecular size of CH_4 and N_2; (d) illustration of the different kinetic effects of CH_4 and N_2 through the window of MIL-120Al. Color code: C, gray; H, white; O, red; Al, cyan; N, blue.

The structure of MIL-120Al was constructed using infinite rod building blocks and BTEC ligands, which exhibits a novel three-dimensional open-framework. Figure 1a shows the rhombic open 1D channels of MIL-120Al were formed along the c-axis and the pore walls were formed by the aromatic ring parallel to the c-axis. The pore diameter was measured to be 5.4×4.7 Å.[40] Obviously, the pore size was slightly larger than the dynamic diameter of CH_4 and N_2 (Figures 1b, 1c), suggesting its potential application for the kinetic separation of CH_4/N_2 (Figure 1d).
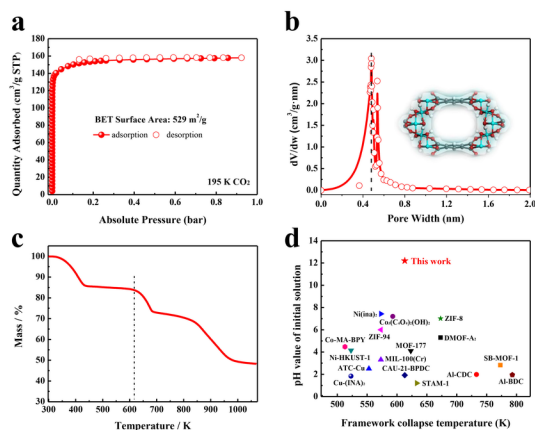

FIGURE 2 (a) CO_2 adsorption and desorption isotherms obtained for MIL-120Al at 195 K; (b) pore size distribution of MIL-120Al; (c) TG curve obtained for MIL-120Al; (d) comparison of the pH value of the initial solution and thermal stability of conventional CH_4/N_2 separation materials.

Limited by the small window diameter, the pore-size of MIL-120Al cannot be obtained using N_2 as a probe (Figure S2). Thus, a carbon dioxide sorption experiment was performed at 195 K, as shown in Figure 2a. The isotherm obtained for MIL-120Al shows a typical type I behavior, indicating its microporous

nature. The Brunauer–Emmett–Teller (BET) surface area and pore volume were 529 m^2/g and 0.24 cm^3/g, respectively. These values were slightly higher than those previously reported, which may be attributed to the sample washing step using high temperature methanol.[44] The pore size distribution was evaluated using the Horvath–Kawazoe model (Figure 2b) and the calculated pore size (4.8 Å) was consistent with the results obtained from the crystal structure (5.4 × 4.7 Å).[40] From a practical point of view, the pH value of the initial solution and thermal stability are two key metrics for evaluating the adsorbent. Figure 2c and Table S1 show MIL-120Al can only be synthesized in an alkaline environment (pH >7) among the conventional CH_4/N_2 separation materials, which means that a conventional stainless-steel reactor can be used in the industrial synthesis of this material. In addition, of TGA (Figures 2c, 2d and Table S1) shows that MIL-120Al exhibits higher thermal stability (613 K) when compared to ATC-Cu (553 K)[12] and Ni(ina)$_2$ (573 K).[27]

3.2 Kinetic and equilibrium adsorption

Single-component CH_4 and N_2 adsorption isotherms of MIL-120Al were measured at 273–313 K and up to 1 bar pressure, as shown in Figure 3a. MIL-120Al shows an obviously preferential adsorption of CH_4 over N_2 at all temperatures studied, especially at low pressure (273 K), indicating its high affinity toward CH_4. Specifically, at 298 K and 1.0 bar, the CH_4 uptake capacity of MIL-120Al was up to 33.7 cm^3/g, which is comparable to the benchmark Al-based MOF Al-CDC (32.0 cm^3/g)[45] and far exceeds other porous materials, such as CAU-21-BPDC (22.2 cm^3/g),[46] Co-MA-BPY (20.6 cm^3/g),[47] SB-MOF-1 (20.6 cm^3/g),[48] and Cu-(INA)$_2$ (18.6 cm^3/g),[49] which demonstrates its extremely high performance for CH_4 capture (Figure 3c). A more comprehensive comparison is given in Table S7 (Supporting information). The corresponding CH_4 volume adsorption uptake of MIL-120Al based on the framework density was calculated to be 52.91 cm^3/cm^3, which also exceeds other previously reported materials (Figure S6 and Table S3) with the exception of NKMOF-8-Me (54.11 cm^3/cm^3).[50] In contrast, MIL-120Al only adsorbs a small amount of N_2 (10.5 cm^3/g) under the same conditions. The repeatability of the adsorption performance was also tested using a cycling experiment. The adsorption of CH_4 over five cycles was maintained at ~33 cm^3/g, proving its excellent reproducibility (Figure S5). To further explore the CH_4/N_2 separation properties of MIL-120Al, the adsorption selectivity's for 50/50 CH_4/N_2 mixtures were predicted using ideal adsorbed solution theory (IAST) (Figure 3b). As shown in Figure 3b, the CH_4/N_2 selectivity for MIL-120Al can reach 6.0 at 298 K and 1 bar, which is higher than other most previously reported MOFs (Table S7 and Figure 3c).[51-53]
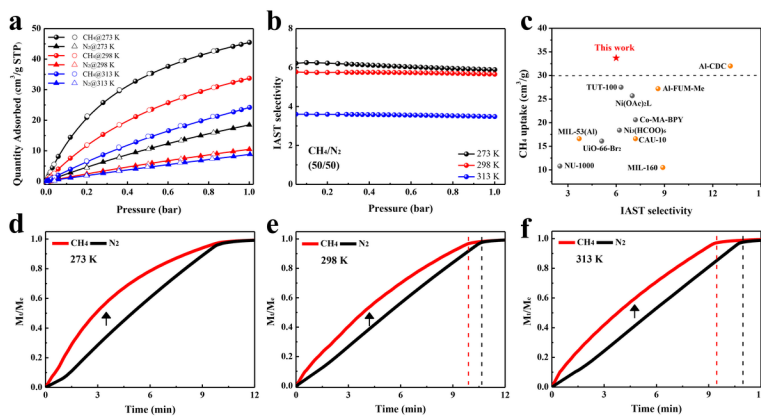

FIGURE 3 (a) CH_4 and N_2 adsorption isotherms obtained for MIL-120Al at different temperatures; (b) IAST selectivity's of MIL-120Al for CH_4/N_2 at 273, 298, and 313 K; (c) a comparison of the IAST selectivity of CH_4/N_2 and CH_4 uptake of MIL-120Al versus those of previously reported water stable benchmark MOFs (orange represents the Al-based MOFs reported in this work); kinetic adsorption profiles obtained for CH_4 and N_2 for MIL-120Al at 273 K (d), 298 K (e), and 313 K (f).

6

Furthermore, due to the comparable kinetic diameters of the gas molecules and pore dimensions, we also investigated the time-dependent adsorption kinetics profiles of MIL-120Al at 263–353 K from 0 to 1.0 bar (Figures 3d–f and S7). Figures 3d–f show that MIL-120Al exhibits a considerably faster uptake of CH_4 than N_2 at the temperatures studied and increasing the temperature gradually increases the difference in the equilibration time between CH_4 and N_2. At 313 K, the time to reach equilibrium for CH_4 was only 9.3 min, while N_2 required 11.1 min. We speculate that the faster diffusion rate of CH_4 than N_2 can be attributed to the non-polar porous walls of MIL-120Al formed by the aromatic rings. It is noteworthy that the faster diffusion rate of CH_4 than N_2 has been observed for the first time in MOFs. This phenomenon is contrary to that of conventional MOF adsorbents, such as NKMOF-8-Me and Al-CDC,[50] in which N_2 always preferentially reaches equilibrium. To quantify the kinetic selectivity of MIL-120Al, the kinetic selectivity $[D(CH_4)/D(N_2)]$ was obtained, and the value was up to 1.8 at 298 K (Table S2). It is reasonable to believe that the kinetic adsorption properties of MIL-120Al will plays a crucial role in CH_4/N_2 separation for practical applications.
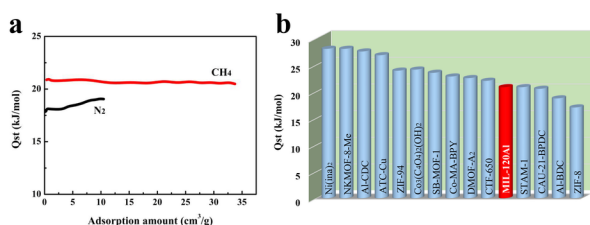

FIGURE 4 (a) CH_4 and N_2 adsorption heat of MIL-120Al calculated using the Clausius–Clapeyron equation; (b) a comparison of the CH_4 adsorption heat observed for some previously reported CH_4-selective materials.

The isoteric heat of adsorption (Q_{st}) for CH_4 and N_2 in the MIL-120Al were calculated based on the single-component adsorption isotherms obtained at 273 and 298 K using the Clausius–Clapeyron equation.[54] Figure 4a shows the Q_{st} at zero coverage for CH_4 (20.87 kJ/mol) was higher than that of N_2 (17.83 kJ/mol), suggesting the stronger interactions formed between the framework and CH_4 molecules. Interestingly, we found that upon increasing the CH_4 loading, the Q_{st} value were smooth lines with almost unchanged values (20.48–20.87 kJ/mol). This implies the energetic homogeneity of the MIL-120Al surface, and a similar phenomenon was also observed in $[Co_3(C_4O_4)_2(OH)_2]$.[1] In addition, when compared with the outstanding materials reported in the literature (see Figure 4b), MIL-120Al exhibits a low initial Q_{st} value for CH_4, which is beneficial to sorbent regeneration in an industrial process.
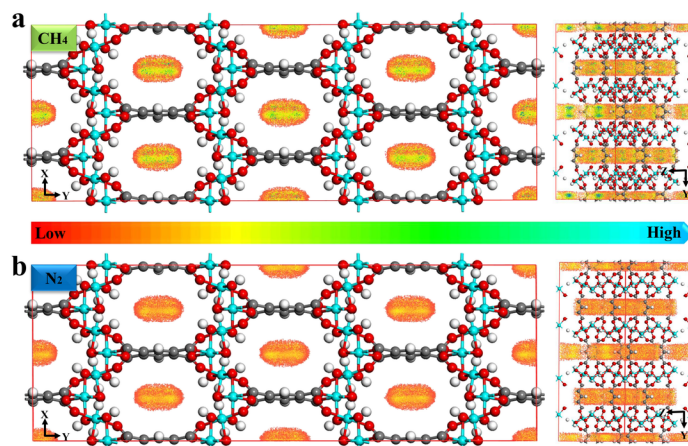
3.3 GCMC calculations

7

FIGURE 5 Contour plots obtained for the center of mass (COM) probability distributions of CH_4 (a) and N_2 (b) in the mixture adsorbed on MIL-120Al at 298 K and 1.0 bar.

Grand canonical Monte Carlo (GCMC) simulations were carried out to give a deeper insight into the separation mechanism of CH_4 and N_2 on MIL-120Al. Figure 5 shows the distribution profiles of CH_4/N_2 at 298 K and 1.0 bar after reaching equilibrium in the MIL-120Al structure. Obviously, the CH_4 molecules prefers to stay in the pore formed between the two aromatic rings. A similar phenomenon has also been reported in the literature,[55] which has proved that CH_4 molecules and the aromatic rings of framework form C-H···π interactions. For N_2, the adsorption sites also stay at the middle of the pore, but the density was much lower than that of CH_4, as confirmed by the probability distributions of the center of mass. The binding energies of CH_4 and N_2 were calculated to be 27.11 and 22.26 kJ/mol, respectively, which is consistent with the trend observed for the experimental Q_{st} values (20.87 vs 17.83 kJ/mol). All of the results obtained using GCMC confirmed that the pore centers of MIL-120Al were the most energetically-favorable binding sites for CH_4, thus exhibiting a superior recognition ability when separating the CH_4/N_2 mixture.

3.4 Breakthrough experiments for an CH_4/N_2 mixture on MIL-120Al
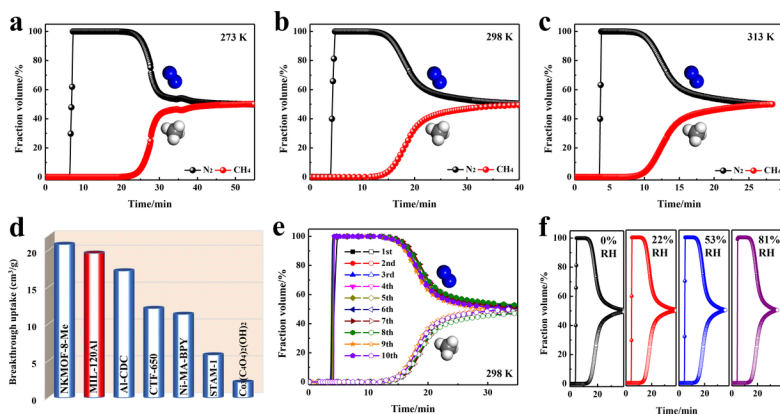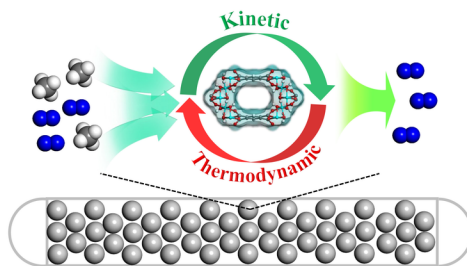

FIGURE 6 Experimental breakthrough curves obtained for MIL-120Al during the separation of CH_4/N_2 (50/50) at 1.0 bar and different temperatures: (a) 273 K, (b) 298 K, and (c) 313 K; (d) a comparison of the

CH_4 breakthrough uptake of MIL-120Al with some selected water stable benchmark materials reported in the literature. (e) The experimental breakthrough cycles for CH_4/N_2 (50/50) separation on MIL-120Al at 298 K and 1.0 bar; (f) breakthrough curves obtained upon varying the humidity of a 50/50 CH_4/N_2 mixture at 298 K and 1.0 bar.

To simultaneously consider the effects of both the thermodynamic and kinetic factors on the separation process, dynamic breakthrough experiments were conducted at 273–313 K using an equimolar CH_4/N_2 mixture (Figure 6). From the results (Figure 6a–c), N_2 first elutes through the column and CH_4 elutes after a certain amount of time, indicating that the CH_4/N_2 mixture can be separated over a wide temperature range from 273 to 313 K using MIL-120Al. In particular, at 298 K and 1 bar, N_2 was found to first flow out of the breakthrough column and can be detected at 4.2 min. CH_4 shows an obvious breakthrough delay behavior and cannot be the detected until 12.2 min. The calculated retention time for CH_4 was three times more than that of N_2, which is comparable to that of Al-CDC under similar test conditions.[45] Considering the moderate IAST and kinetic selectivity of MIL-120Al at 298 K, we believe that the excellent separation of CH_4/N_2 on MIL-120Al was controlled by the synergistic effect of the thermodynamic and kinetic factors (Scheme 1). From the calculations using these breakthrough results (Figure 6d and Table S8), the loading of CH_4 enriched from the mixture was ˜19.6 cm^3/g, which is comparable to that of the best materials reported in the literature, e.g., NKMOF-8-Me (20.8 cm^3/g),[50] and higher than that of all previously reported MOFs. For a low concentration of CH_4 inlet gas (20/80 and 10/90 CH_4/N_2), it is also feasible to realize the good separation of CH_4 from N_2 using MIL-120Al (Figure S12 and S13). In addition, as revealed using multiple breakthrough experiments, the separation time of MIL-120Al can be maintained after 10 cycles, implying its good reusability (Figure 6e). From a practical viewpoint, the effect of H_2O in the enrichment process of low-concentration CMM should also be considered,[56] thus, breakthrough experiments were performed using the CH_4/N_2 (50/50) mixture with humidity in the range of 22–81% RH. Figure 6f shows the retention time of N_2 and CH_4 were similar to those observed in a dry environment even under 81% RH, indicating that the separation performance of this material was not significantly affected by the presence of H_2O.

SCHEME 1 Illustration of the CH_4/N_2 separation process in the adsorption column filled with MIL-120Al.

3.5 PSA simulations

A simulated PSA process model was designed to evaluate the application potential of MIL-120Al in an industrial separation process. Using this model, the purity, recovery, and productivity of CH_4 at different feed gas flow rates and/or adsorption times were investigated. Figure 7 shows the CH_4 purity and productivity increases with an increase of in the feed gas flow rate. At the same time, a high gas flow rate leads to an increase in the amount of unabsorbed CH_4, thus resulting in a decreased recovery rate. When setting the

pass line for the CH$_4$ recovery rate at 80%, the pristine 50% CH$_4$ mixture can be enriched to 86% with a high productivity of 1.54 mol/h/Kg (Table S12). Such a high CH$_4$ recovery and purity demonstrate that MIL-120Al has a good enrichment effect for the CH$_4$/N$_2$(50/50) mixture. As another important factor, the adsorption time was also considered in the simulation. An appropriate prolongation of the adsorption time was beneficial to increasing the recovery and productivity of CH$_4$ (Table S13). For a 20/80 CH$_4$/N$_2$ inlet gas mixture, as shown in Figure S16, it can also achieve a 59% product gas concentration using this PSA method (Tables S10, S11). All of these results indicate that MIL-120Al has great application potential for CH$_4$/N$_2$ separation.
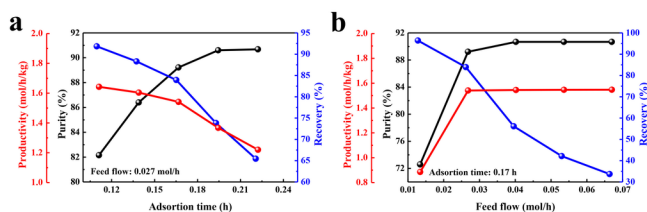

FIGURE 7 Purity, recovery, and productivity of CH$_4$ using a PSA simulation with a CH$_4$/N$_2$ (50/50) feed gas mixture at different adsorption time (a) and feed flow rates (b).

3.6 Large-scale synthesis and structural stability of MIL-120Al

For industrial application, the structural stability and scalable synthesis of the adsorbent also should be considered besides its adsorption performance. Figure S15 and S19a show the variable temperature PXRD patterns and corresponding 77 K N$_2$adsorption isotherms, which reveal that MIL-120Al exhibits excellent thermal stability up to 523 K without any phase changes being observed. Furthermore, the chemical stability of MIL-120Al toward organic solvents and acid-base environments was also investigated (Figure S19b and Figure S19c). The framework of MIL-120Al was stable under extreme conditions for several hours, and no loss in its crystallinity and no phase changes were observed in PXRD and the 77 K N$_2$ adsorption isotherms. In addition, when compared with the pristine material, the PXRD patterns remain unchanged after the adsorption and breakthrough tests, indicating its good test stability (Figure S19d). More importantly, MIL-120Al was easily synthesized from very common chemical commodities via a 'green' and scalable method, in which the only solvent was water (Figures 8a, 8b). In addition, the almost consistent breakthrough curves observed for the large-scale sample with that of the laboratory-scale indicate that the scale-up synthesis does not have a negative effect on the separation properties of the material (Figure 8c).
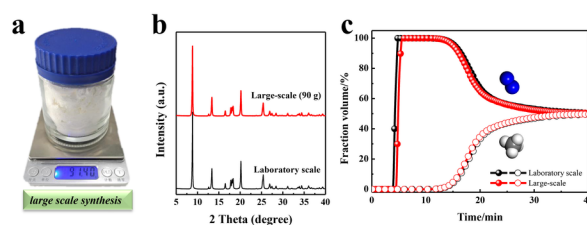
FIGURE 8 (a) 91.40 g of MIL-120Al synthesized using a 2 L reactor; (b) PXRD patterns of MIL-120Al Laboratory scale and large-scale samples; (c) breakthrough curves obtained for MIL-120Al on different scales for an equimolar binary mixture of CH_4/N_2 at 298 K and 1 bar.

4 CONCLUSIONS

In summary, we have reported an ultra-microporous aluminum-based MOF with unique porous walls constructed from benzene rings with a suitable pore size to capture CH_4 from a CH_4/N_2 mixture. The framework material exhibited a high CH_4 uptake (33.7 cm^3/g) along with satisfactory CH_4/N_2 selectivity (6.0). Benefiting from a thermodynamic-kinetic synergistic separation effect, this MOF shows excellent separation performance for CH_4/N_2 mixtures under dynamic conditions, which is comparable to that of a previously reported benchmark CH_4/N_2 adsorbent (Al-CDC), as demonstrated by our breakthrough experiments. Meanwhile, the CH_4 breakthrough uptake of MIL-120Al (19.6 cm^3/g) is also higher than most of the previously reported water stable materials. More importantly, further PSA simulations indicated that after a one-step enrichment, pristine 50% methane can be enriched to 86%, and the CH_4 recovery and productivity can reach up to 80% and 1.54 mol/h/Kg, respectively. When combined with the good enrichment effect of the PSA simulation, the stable structure, easily scaled-up production, and regenerability of MIL-120Al demonstrate its promising potential as an adsorbent for CH_4/N_2 separation. This work not only presents a efficient performance adsorbent for low-concentration CMM enrichment, but also provides useful guidance for the design and preparation of novel CH_4/N_2 separate adsorbents.

AUTHOR CONTRIBUTIONS

Feifei Zhang : Conceptualization (equal); funding acquisition (equal); investigation (equal); writing–original draft (equal).**Hua Shang** : Data curation (equal); investigation (equal).**Bolun Zhai** : Data curation (equal); investigation (equal).**Xiaoming Li** : Formal analysis (equal). **Yingying Zhang** : Formal analysis (equal). **Xiaoqing Wang** : Formal analysis (equal). **Jinping Li** : Resources (equal); supervision (equal).**Jiangfeng Yang** : Conceptualization (equal); funding acquisition (equal); resources (equal); writing–review and editing (equal).

ACKNOWLEDGMENTS

CONFLICT OF INTEREST

The authors declare that they have no known competing financial interests or personal relationships that could appear to influence the work reported in this paper.

DATA AVAILABILITY STATEMENT

The data that support the findings of this study are available from the corresponding author.

ORCID

Jinping Li (*https://orcid.org/0000-0002-2628-0376*)

Jiangfeng Yang (*https://orcid.org/0000-0003-0135-2203*)

REFERENCES

1. Li L, Yang L, Wang J, et al. Highly efficient separation of methane from nitrogen on a squarate-based metal organic framework. *AlChE J* . 2018; 64:3681-3689.
2. Chang M, Zhao Y, Yang Q, Liu D. Microporous Metal-Organic Frameworks with Hydrophilic and Hydrophobic Pores for Efficient Separation of CH_4/N_2 Mixture. *ACS Omega* . 2019; 4:14511-14516.
3. He Y, Zhou W, Qian G, Chen B. Methane storage in metal-organic frameworks. *Chem Soc Rev* . 2014; 43:5657-5678.
4. Saha D, Grappe HA, Chakraborty A, Orkoulas G. Postextraction Separation, On-Board Storage, and Catalytic Conversion of Methane in Natural Gas: A Review. *Chem Rev* . 2016; 116:11436-11499.
5. Chu S, Majumdar A. Opportunities and challenges for a sustainable energy future. *Nature* 2012; 488: 294-303.
6. Limbri H, Gunawan C, Rosche B, Scott J. Challenges to Developing Methane Biofiltration for Coal Mine Ventilation Air: A Review.*Water Air Soil Pollut* . 2013; 224:1-15.
7. Kim J, Maiti A, Lin L, Stolaroff JK, Smit B, Aines RD. New materials for methane capture from dilute and medium-concentration sources.*Nat Commun* . 2013; 4:1694.
8. Guo Y, Hu J, Liu X, Sun T, Zhao S, Wang S. Scalable solvent-free preparation of $Ni_3(HCOO)_6$ frameworks for highly efficient separation of CH_4 from N_2. *Chem Eng J* . 2017; 327:564-572.
9. Qadir S, Gu Y, Ali S, et al. A thermally stable isoquinoline based ultra-microporous metal-organic framework for CH_4separation from coal mine methane. *Chem Eng J.* 2022; 428:131136.
10. Du S, Wu Y, Wang X, et al. Facile synthesis of ultramicroporous carbon adsorbents with ultra-high CH_4 uptake by in situ ionic activation. *AlChE J.* 2020; 66:e16231.
11. Hu J, Sun T, Liu X, Zhao S, Wang S. Rationally tuning the separation performances of $[M_3(HCOO)_6]$ frameworks for CH_4/N_2 mixtures via metal substitution. *Microporous Mesoporous Mater* . 2016; 225: 456-464.
12. Niu Z, Cui X, Pham T, et al. A Metal-Organic Framework Based Methane Nano-trap for the Capture of Coal-Mine Methane. *Angew Chem Int Ed* . 2019; 58:10138-10141.
13. Yang J, Li J, Wang W, Li L, Li J. Adsorption of CO_2, CH_4, and N_2 on 8-, 10-, and 12-Membered Ring Hydrophobic Microporous High-Silica Zeolites: DDR, Silicalite-1, and Beta. *Ind Eng Chem Res.* 2013; 52:17856-17864.
14. Wang X, Li L, Yang J, Li J. $CO_2/CH_4$and CH_4/N_2 separation on isomeric metal organic frameworks. *Chin J Chem Eng.* 2016; 24:1687-1694.
15. Wang K, Li C, Liang Y, et al. Rational construction of defects in a metal-organic framework for highly efficient adsorption and separation of dyes. *Chem Eng J.* 2016; 289:486-493.
16. Furukawa H, Cordova KE, O'Keeffe M, Yaghi OM. The Chemistry and Applications of Metal-Organic Frameworks. *Science* 2013; 341:974-986.
17. Lu W, Wei Z, Gu Z, et al. Tuning the structure and function of metal-organic frameworks via linker design. *Chem Soc Rev* . 2014; 43:5561-5593.
18. Bao Z, Chang G, Xing H, Krishna R, Ren Q, Chen B. Potential of microporous metal-organic frameworks for separation of hydrocarbon mixtures, *Energy Environ. Sci* . 2016; 9:3612-3641.
19. Zhai Q, Bu X, Zhao X, Li D, Feng P, Pore Space Partition in Metal-Organic Frameworks. *Acc Chem Res.* 2017; 50:407-417.

20. Li JR, Sculley J, Zhou HC. Metal-Organic Frameworks for Separations.*Chem Rev* . 2012; 112: 869-932.

21. Yu J, Xie L, Li J, Ma Y, Seminario JM, Balbuena PB. CO_2 Capture and Separations Using MOFs: Computational and Experimental Studies. *Chem Rev* . 2017; 117:9674-9754.

22. Adil K, Belmabkhout Y, Pillai RS, et al. Gas/vapour separation using ultra-microporous metal-organic frameworks: insights into the structure/separation relationship. *Chem Soc Rev* . 2017; 46:3402-3430.

23. Yang Q, Liu D, Zhong C, et al. Development of Computational Methodologies for Metal-Organic Frameworks and Their Application in Gas Separations. *Chem Rev* . 2013; 113:8261-8323.

24. Wang Y, Huang N, Zhang X, et al. Selective Aerobic Oxidation of a Metal-Organic Framework Boosts Thermodynamic and Kinetic Propylene/Propane Selectivity. *Angew Chem Int Ed* . 2019; 58:7692-7696.

25. Bachman JE, Kapelewski MT, Reed DA, Gonzalez MI, Long JR. M_2(m-dobdc) (M = Mn, Fe, Co, Ni) Metal-Organic Frameworks as Highly Selective, High-Capacity Adsorbents for Olefin/Paraffin Separations. *J Am Chem Soc.* 2017; 139:15363-15370.

26. Hao H, Zhao Y, Chen D, et al. Simultaneous Trapping of C_2H_2 and C_2H_6 from a Ternary Mixture of $C_2H_2/C_2H_4/C_2H_6$in a Robust Metal-Organic Framework for the Purification of C_2H_4. *Angew Chem Int Ed.* 2018; 57:16067-16071.

27. Wang S, Shivanna M, Yang Q. Nickel-Based Metal-Organic Frameworks for Coal-Bed Methane Purification with Record CH_4/N_2 Selectivity. *Angew Chem Int Ed* . 2022; 61:e17819.

28. Chang M, Yan T, Wei Y, Wang J, Liu D, Chen J. Enhancing CH_4 Capture from Coalbed Methane through Tuning van der Waals Affinity within Isoreticular Al-Based Metal-Organic Frameworks. *ACS Appl Mater Interfaces* 2022; 14:25374-25384.

29. Gaab M, Trukhan N, Maurer S, Gummaraju R, Mueller U. The progression of Al-based metal-organic frameworks - From academic research to industrial production and applications. *Microporous Mesoporous Mater* . 2012; 157:131-136.

30. Chen Y, Wang Y, Wang Y, et al. Improving CH_4 uptake and CH_4/N_2 separation in pillar-layered metal-organic frameworks using a regulating strategy of interlayer channels. *AlChE J* . 2022; e17819.

31. Li L, Lin R, Wang X, et al. Kinetic separation of propylene over propane in a microporous metal-organic framework. *Chem Eng J* . 2018; 354:977-982.

32. Ding Q, Zhang Z, Yu C, et al. Exploiting equilibrium-kinetic synergetic effect for separation of ethylene and ethane in a microporous metal-organic framework. *Sci Adv* . 2020;6:eaaz4322.

33. Bereciartua PJ, Corma A, Jorda JL,et al.Control of zeolite framework flexibility and pore topology for separation of ethane and ethylene.*Science* 2017; 358:1068-1071.

34. Lee CY, Bae YS, Jeong NC, et al. Kinetic Separation of Propene and Propane in Metal-Organic Frameworks: Controlling Diffusion Rates in Plate-Shaped Crystals via Tuning of Pore Apertures and Crystallite Aspect Ratios. *J Am Chem Soc* . 2011; 133:5228-5231.

35. Lyndon R, You W, Ma Y, et al. Tuning the Structures of Metal–Organic Frameworks via a Mixed-Linker Strategy for Ethylene/Ethane Kinetic Separation. *Chem Mater* . 2020; 32:3715-3722.

36. Zeng H, Xie M, Wang T, et al. Orthogonal-array dynamic molecular sieving of propylene/propane mixtures. *Nature* 2021; 595:542-548.

37. Cadiau A, Adil K, Bhatt PM, Belmabkhout Y, Eddaoudi M. A metal-organic framework-based splitter for separating propylene from propane.*Science* 2016; 353:137-140.

38. Yu L, Han X, Wang H, et al. Pore Distortion in a Metal–Organic Framework for Regulated Separation of Propane and Propylene. *J Am Chem Soc* . 2021; 143:19300-19305.

39. Liang B, Zhang X, Xie Y, et al. An Ultramicroporous Metal–Organic Framework for High Sieving Separation of Propylene from Propane.*J Am Chem Soc* . 2020; 142:17795-17801.

40. Volkringer C, Loiseau T, Haouas M, et al. Occurrence of Uncommon Infinite Chains Consisting of Edge-Sharing Octahedra in a Porous Metal Organic Framework-Type Aluminum Pyromellitate $Al_4(OH)_8C_{10}O_8H_2$(MIL-120): Synthesis, Structure, and Gas Sorption Properties.*Chem Mater* . 2009; 21:5783-5791.

41. Perdew JP, Burke K, Ernzerhof M. Generalized Gradient Approximation Made Simple. *Phys Rev Lett* . 1996; 77:3865-3868.

42. Yang J, Bai H, Shang H, Wang J, Li J, Deng S. Experimental and simulation study on efficient CH_4/N_2 separation by pressure swing adsorption on silicalite-1 pellets. *Chem Eng J* . 2020; 388:124222.
43. Liu J, Shang H, Yang J, Wang J, Li J, Deng S. Novel zeolite/carbon monolith adsorbents for efficient CH_4/N_2 separation. *Chem Eng J* . 2021; 426:130163.
44. Zhang P, Zhong Y, Yao Q, et al. Robust Ultramicroporous Metal-Organic Framework with Rich Hydroxyl-Decorated Channel Walls for Highly Selective Noble Gas Separation. *J Chem Eng Data* 2020; 65:4018-4023.
45. Chang M, Zhao Y, Liu D, Yang J, Li J, Zhong C. Methane-trapping metal-organic frameworks with an aliphatic ligand for efficient CH_4/N_2 separation. *Sustain Energy Fuels* 2020; 4:138-142.
46. Lv D, Wu Y, Chen J, et al. Improving CH_4/N_2 selectivity within isomeric Al-based MOFs for the highly selective capture of coal-mine methane. *AlChE J* . 2020; 66:e16287.
47. Liu X, Gu Y, Sun T, et al. Water Resistant and Flexible MOF Materials for Highly Efficient Separation of Methane from Nitrogen. *Ind Eng Chem Res* . 2019; 58:20392-20400.
48. Chang M, Ren J, Yang Q, Liu D. A robust calcium-based microporous metal-organic framework for efficient CH_4/N_2 separation. *Chem Eng J* . 2021; 408:127294.
49. Hu J, Sun T, Liu X, Guo Y, Wang S. Separation of CH_4/N_2 mixtures in metal-organic frameworks with 1D micro-channels. *RSC Adv* . 2016; 6:64039-64046.
50. Chang M, Wang F, Wei Y, et al. Separation of CH_4/N_2 by an ultra-stable metal-organic framework with the highest breakthrough selectivity. *AlChE J* . 2022; 68:e17794.
51. Shi Q, Wang J, Shang H, et al. Effective CH_4 enrichment from N_2 by SIM-1 via a strong adsorption potential SOD cage. *Sep Purif Technol* . 2020; 230:115850.
52. Kim MB, Thallapally PK. Effective CH_4/N_2 separation using NU-1000 at high pressures. *J Coord Chem* . 2021; 74:216-225.
53. Saha D, Deng S. Structural Stability of Metal Organic Framework MOF-177. *J Phys Chem Lett* . 2010; 1:73-78.
54. Chen Q, Luo M, Hammershoj P, et al. Microporous Polycarbazole with High Specific Surface Area for Gas Storage and Separation. *J Am Chem Soc* . 2012; 134:6084-6087.
55. Li T, Jia X, Chen H, et al. Tuning the Pore Environment of MOFs toward Efficient CH_4/N_2 Separation under Humid Conditions. *ACS Appl Mater Interfaces* 2022; 14:15830-15839.
56. Liu J, Tang X, Liang X, et al. Superhydrophobic zeolitic imidazolate framework with suitable SOD cage for effective CH_4/N_2 adsorptive separation in humid environments. *AlChE J* . 2022; 68:e17589.

SUPPORTING INFORMATION

Additional supporting information may be found online in the Supporting Information section at the end of this article.

Hosted file

Supporting Information.docx available at https://authorea.com/users/519636/articles/593291-thermodynamic-kinetic-synergistic-separation-of-ch4-n2-on-a-robust-aluminum-based-metal-organic-framework

Hosted file

Graphical Abstract.docx available at https://authorea.com/users/519636/articles/593291-thermodynamic-kinetic-synergistic-separation-of-ch4-n2-on-a-robust-aluminum-based-metal-organic-framework